Met. Mater. Int., Vol. 23, No. 6 (2017), pp. 1197~1203
doi: 10.1007/s12540-017-6922-3

Characteristics of Copper-Clad Aluminum Rods Prepared by Horizontal Continuous Casting

Yubo Zhang[1*], Ying Fu[1,2*], Jinchuan Jie[1], Li Wu[1], Kateryna Svynarenko[1], Qingtao Guo[3], Tingju Li[1], and Tongmin Wang[1]

[1]School of Materials Science and Engineering, Dalian University of Technology, Dalian 116024, China
[2]Engineering Institute, Bohai University, Jinzhou 121001, China
[3]State Key Laboratory of Metal Material for Marine Equipment and Application, Anshan 114000, China

(received date: 28 December 2016 / accepted date: 13 April 2017)

An innovative horizontal continuous casting method was developed and successfully used to prepare copper-clad aluminum (CCA) rods with a diameter of 85 mm and a sheath thickness of 16 mm. The solidification structure and element distribution near the interface of the CCA ingots were investigated by means of a scanning electron microscope, an energy dispersive spectrometer, and an electron probe X-ray microanalyzer. The results showed that the proposed process can lead to a good metallurgical bond between Cu and Al. The interface between Cu and Al was a multilayered structure with a thickness of 200 μm, consisting of Cu_9Al_4, $CuAl_2$, α-Al/$CuAl_2$ eutectic, and α-Al + α-Al/$CuAl_2$ eutectic layers from the Cu side to the Al side. The mean tensile-shear strength of the CCA sample was 45 MPa, which fulfills the requirements for the further extrusion process. The bonding and diffusion mechanisms are also discussed in this paper.

Keywords: composites, casting, interfaces, mechanical properties, computer simulation

1. INTRODUCTION

Bimetallic cladding materials have been widely used in many industrial fields because of their superior characteristics resulting from the difference in the physical, chemical, and mechanical properties of the constituent alloys. In addition, these materials are more economical than their monometallic components [1,2]. For example, Cu is a common material used in electrical applications because of its excellent conductivity. However, the resource shortage and high price of copper impose serious constraints on its widespread application. An alternative to the conventional Cu alloys used in electric transmission is copper-clad aluminum (CCA). The use of CCA could reduce the weight by 50% and decrease the cost by 30%-40% as compared to Cu alloys with equivalent conductivity [1].

With the increasing application of bimetallic cladding materials in the manufacturing, military, and aerospace industries, recent years have seen a growing interest in the preparation of these materials. Many methods such as roll/press bonding [3,4], explosion welding [5], diffusion bonding [6], and casting [7,8] are reported for the production of different bimetallic materials. Among these, CCA materials have only been produced by the rolling bonding, overlay welding, and continuous casting methods [9,10]. Continuous casting is considered the optimal method for preparing CCA materials because of its high efficiency and low cost [11-14]. Neumann [15] first invented a vertical core-filling continuous casting (VCFC) method to fabricate various metal cladding materials, including CCA ingots. Su *et al.* [16,17] developed a novel method for horizontal core-filling continuous casting (HCFC) and successfully fabricated CCA rods with a diameter of 30 mm and Cu layer thickness of 3 mm.

In this study, CCA rods with a diameter of 85 mm and a sheath thickness of 16 mm were fabricated by an optimized horizontal continuous casting method. The design of the pouring system was improved by adopting shorter runners, which provided better control in terms of temperature fluctuations and ensured stable efficiency of the casting process. In addition, a compound mold with a complicated structure was replaced with an integral one, which can be prepared by an effective and low-cost process from a single block of graphite. Because of its high melting point, copper was first poured into the mold and shaped, followed by the pouring and combining of the Al melt with the solidified clad-Cu shell. Adequate re-melting and sufficient element diffusion at the interface are necessary for a good metallurgical bonding. The experimental parameters were determined according to simulation results

*Corresponding authors: ybzhang@dlut.edu.cn, fuying_work@sina.com

and previous experiments. The microstructure, composition distribution, and tensile-shear strength of the interfacial region were systematically investigated to analyze the bonding mechanism of Al and Cu.

2. EXPERIMENTAL PROCEDURE

2.1. Experimental process

Figure 1 shows the schematic illustration of the continuous casting equipment used in the production of the CCA rods, which comprises a melting device (for Al and Cu, respectively), graphite mold, cooling device (1st and 2nd water cooling), and withdrawing device. All the experimental parameters were determined based on the numerical results and previous work [18-20].

99.7% pure Cu and 99.9% pure Al were melted in the respective fusion furnaces. All compositions quoted in this work are in wt% unless otherwise stated. When the temperature reached the set value, the Cu melt was poured into the outer part of the mold. During the first water cooling stage, the melt was rapidly solidified and shaped. After the mold was filled, the withdrawal device slowly extruded the Cu tube. In the meantime, the Al melt was poured into the inner part of the mold. Once Al came into contact with the outer shell of Cu, re-melting of the Cu surface occurred to form a metallurgical bond. The casting speed was then increased to a constant value until the process was completed.

After preparation, the CCA rod was cross-cut, ground, and polished for macro- and microscopic observations. An MEF-4A optical microscope (Leica Microsystems GmbH, Germany), a Zeiss Supra55 FE-SEM with EDAX EDS (Zeiss AG, Germany), and an electron probe microanalyzer EPMA-1600 with EDS (Shimadzu Corp., Japan) was used to investigate the microstructure of the interface. All the phase compositions in this study were confirmed by EDS analysis. In order to evaluate the interfacial strength, the specimens were

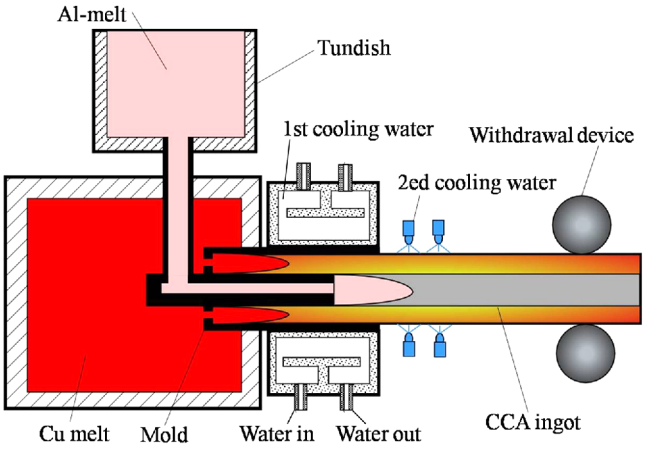

Fig. 1. Schematic illustration of the continuous casting device for CCA rods.

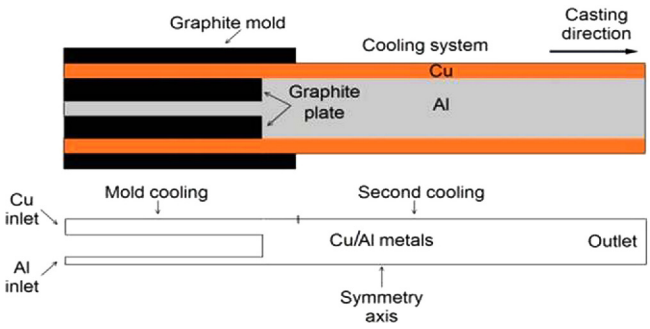

Fig. 2. Calculation model in FLUENT for the Cu/Al clad ingot.

cut lengthwise from the as-cast clad ingot for tensile-shear testing. The tests were performed using a ZwickBZ2.5/TS1S machine at a velocity of 1 mm·min^{-1}.

2.2. Numerical simulation

The key to fabricating CCA rods by horizontal continuous casting is to control the reaction between Al and Cu. On the one hand, the reaction should proceed sufficiently to form a good metallurgical bond, which requires the Al melt to be well filled into the pre-solidified Cu tube at an appropriate temperature. On the other hand, the reaction should not be excessive to avoid breakage of the Cu layer due to superfluous re-melting. Several parameters, including the pouring temperature, casting speed, and cooling water consumption, affect the Al-Cu interfacial reaction to different degrees. Therefore, it is of particular importance to determine the optimal parameters for controlling the reaction.

Based on the commercial finite volume package FLUENT, a comprehensive mathematical model (Fig. 2) was developed to describe the casting process and to reveal the influence of the casting parameters on the temperature and liquid fraction distribution in the CCA rods. In order to simplify the calculation, the axial symmetry model was used, and the following assumptions were made:

(1) The molten Al and Cu behave as an incompressible fluid

(2) The effect of the liquid surface fluctuation in the fluid flow is negligible

(3) The interface reaction between Al and Cu is negligible

(4) There is no diffusion in the solid phase

Then, the boundary conditions can be described as follows:

(1) The velocity boundary condition is used in the inlet and outlet region, and the temperatures at the inlet and outlet boundaries are set to the casting temperature and room temperature, respectively.

(2) The symmetry axis boundary is set to the axisymmetric boundary condition.

(3) The mold cooling and second cooling boundaries are treated as Cauchy-type boundary conditions, and their heat transfer coefficients are determined by the different cooling conditions.

Table 1. Physical properties and constants used in the numerical simulation

Items	Al	Cu
Density ($kg \cdot m^{-3}$)	2700	8900
Viscosity (Pa·s)	0.0029	0.0033
Specific heat capacity ($J \cdot kg^{-1} \cdot K^{-1}$)	900	385
Heat coefficient ($W \cdot m^{-1} \cdot K^{-1}$)	238	390
Latent heat ($kJ \cdot kg^{-1}$)	389	203
Melting point (K)	933	1356.4

After some of the complex boundary conditions are simplified, the model consists of the Cu tube, the graphite mold, an Al filler, a hollow graphite core, and a water cooling system. The physical properties and constants for Al and Cu used in the calculation are listed in Table 1.

3. RESULTS AND DISCUSSION

3.1. Numerical simulation results

Figure 3 shows the simulation results regarding the effect of the casting speed on the temperature and liquid fraction distribution during the stable period of continuous casting. It is clear from the results that the casting speed has a profound influence on the distribution of the temperature. When the casting speed is low (120 mm/min), both melts, Al and Cu, have sufficient time to solidify. Liquid Al is mainly distributed near the exit of the inner mold. The temperature of both Cu and Al when they come into contact with each other is about 1000 K (727 °C); at this temperature Cu is solid and Al is liquid). The interdiffusion proceeds slowly at this temperature, and the interfacial region quickly solidifies, making these conditions unfavorable for a stable metallurgical bond.

At a higher casting speed (200 mm/min), the temperature of Al inside the mold increases and the liquid regions of both Al and Cu appear larger and deeper. The contact temperature of Cu and Al at the end of the inner mold is 1100 K (827 °C) and 1000 K (727 °C), respectively. At this point, Cu solidifies to form a solid shell. In addition, the temperature of the Al melt is high enough for the Al atoms to diffuse into the Cu layer, resulting in a good metal bond. Hence, these temperatures are considered optimal for the Al-Cu reaction and diffusion.

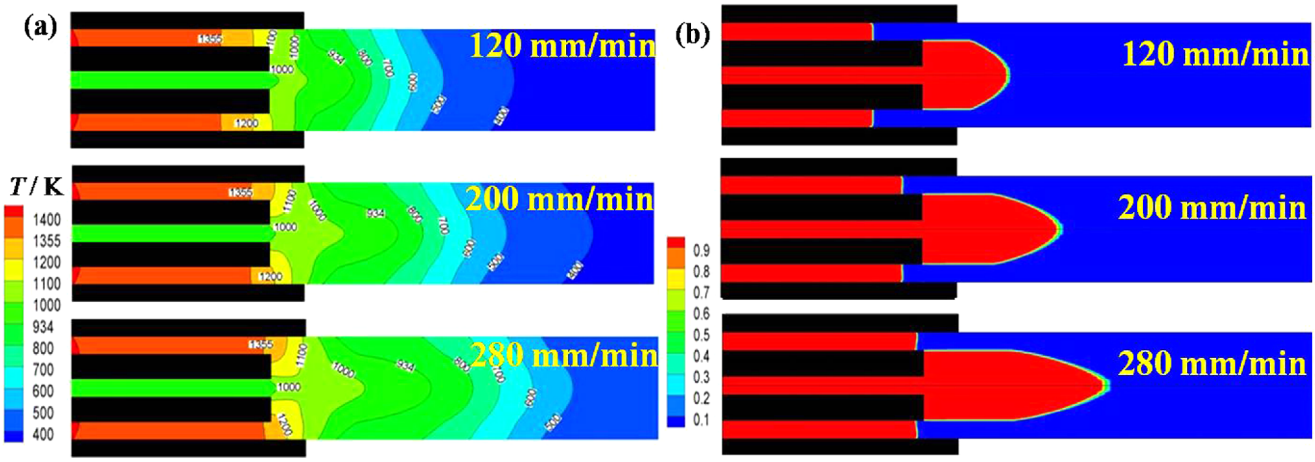

Fig. 3. Effect of different casting speeds on the (a) temperature and (b) liquid fraction distribution in the CCA rods.

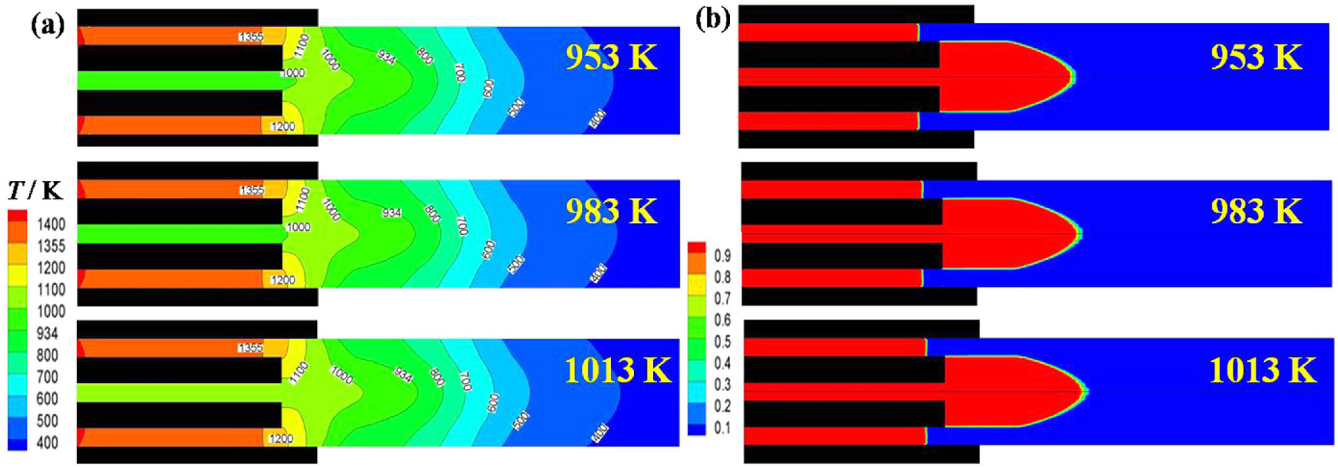

Fig. 4. Effect of different Al pouring temperatures on the (a) temperature and (b) liquid fraction distribution in the CCA rods.

Table 2. Experimental parameters of continuous casting

Parameter	Value
Casting temperature of Al (T_1)/K(°C)	983(710)
Casting temperature of Cu (T_2)/ K(°C)	1423(1150)
Casting speed (v_c)/mm·min^{-1}	200
First cooling water flow rate (Q)/L·h^{-1}	1500-1700
Second cooling water flow rate (Q)/L·h^{-1}	2500

A casting speed of 280 mm/min is too high to form a stable shell of solidified Cu. Moreover, the temperature of Cu and Al at the contact point is about 1355 K (1068 °C) and 1100 K (827 °C), respectively, which accelerates the interdiffusion between these metals. When excessive Al atoms diffuse into the Cu solid, the melting point decreases significantly due to the composition transformation from pure Cu to a Cu-Al alloy. As a result, the Cu layer is easily re-melted or even broken, which leads to failure.

The dependence of the temperature and liquid fraction distribution on the Al pouring temperature is illustrated in Fig. 4. This suggests that the influence of this parameter is not as significant as that of the casting speed. Nevertheless, a difference in the temperature distribution can be found in the Al-Cu contact region. Since the contact temperature directly affects the reaction, the pouring temperature of Al also has a notable effect on the interfacial bonding. Based on the results, 983 K is considered the optimal temperature for the Al melt. Other experimental parameters (Table 2) were set based on the simulation and previous work.

3.2. Microstructure of the interface

The CCA rod prepared by continuous casting, and its cross section (diameter 85 mm, sheath thickness 16 mm) are shown in Figs. 5(a) and 5(b). A clear interface without any evidence of superfluous re-melting of Cu, inclusions, or casting defects such as cracks or cavities can be seen from the macrostructure (Fig. 5(b)), indicating a good metallurgical bond between Cu and Al. The microstructure of the interfacial region marked in Fig. 5(b) is shown in Fig. 5(c). It is a multilayered structure that consists of four layers. In order to confirm the phase composition, EDS analysis of the different IMCs and phases was performed (Table 3). Some regions marked in Fig. 5(c) were

Table 3. Elemental analysis results of the Al/Cu interfaces

Position	Element (atomic%) Al	Cu	Suggested IMCs
1	0	100	Cu
2	65.42	34.58	$CuAl_2$
3	97.20	2.80	α-Al
4	67.16	32.84	$CuAl_2$
5	68.23	31.77	eutectic $CuAl_2$
6	93.74	6.26	eutectic Al

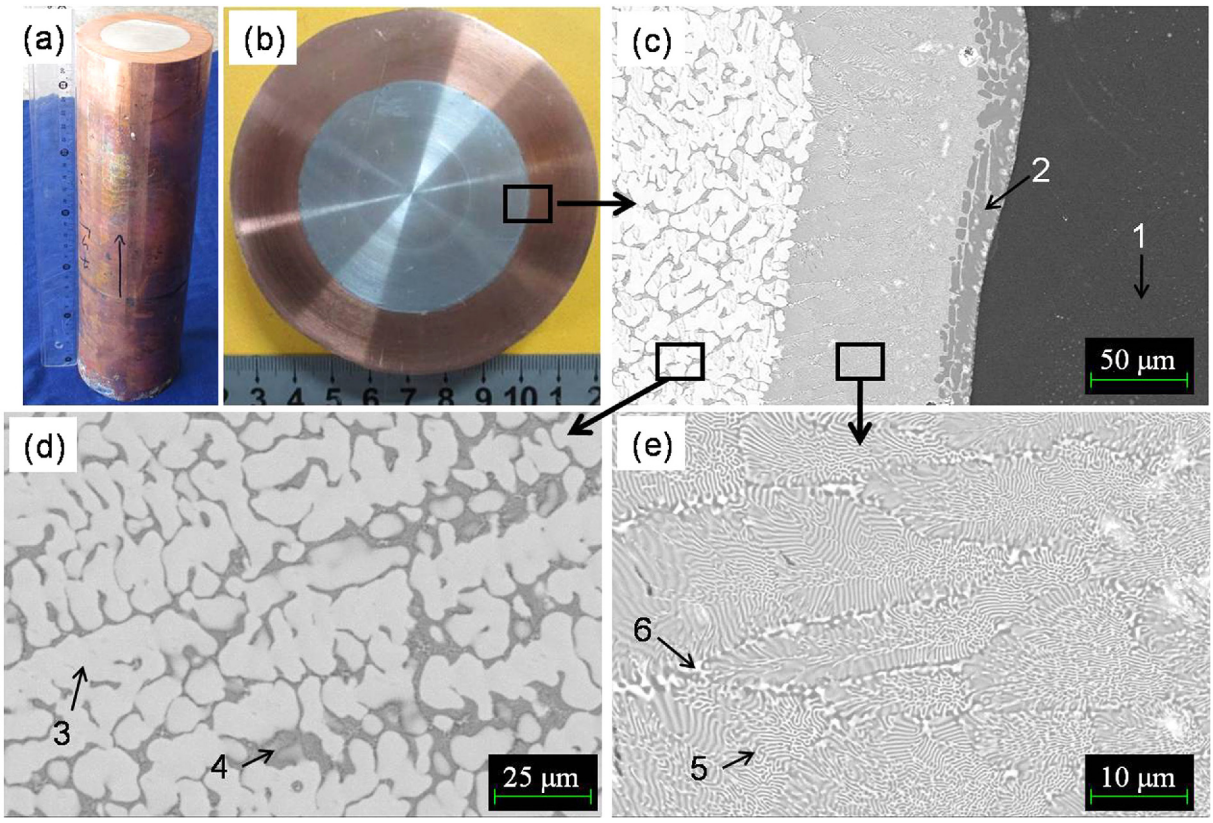

Fig. 5. The (a) CCA ingot, (b) cross-section macrostructure, and (c-e) the magnified interfacial region.

magnified and are shown in Figs. 5(d) and 5(e). The results indicate that the four layers on the CCA interface from the Cu side to the Al side are pure Cu, $CuAl_2$, eutectic (α-Al + $CuAl_2$), and α-Al + eutectic (α-Al + $CuAl_2$).

The outermost layer (darkest part in Fig. 5(c)) is pure Cu, which solidifies first and forms a stable shell before contact with the liquid Al. The next layer, with a thickness of 15-25 μm, is formed by a block-like $CuAl_2$ phase. The third layer from the Cu side (Fig. 5(e)) exhibits a fibrousstructure, which is identified as eutectic (α-Al + $CuAl_2$). The thickness of this layer is about 80 μm. The last layer consists of α-Al and eutectic (α-Al + $CuAl_2$). Since at the time of interaction, Al is in the liquid state while the latter is already solidified, diffusion of the Cu element in the liquid Al is facilitated to a greater extent as compared to that of Al in solid Cu. Hence, the depth of the Cu diffusion layer toward the Al side is greater than that of the Al toward the Cu side.

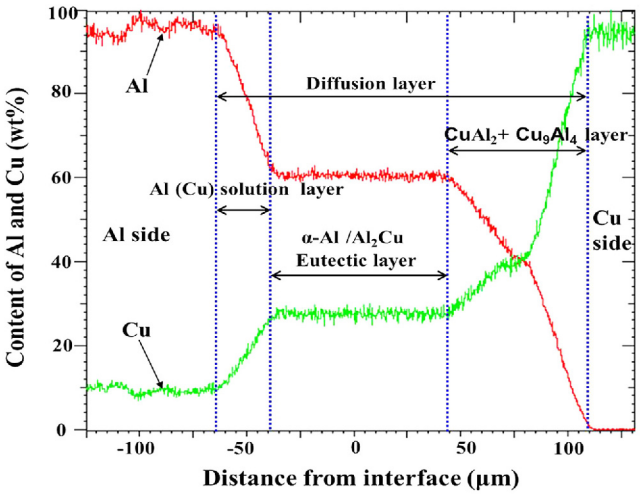

Fig. 7. Line distribution of alloying elements at the interface.

3.3. Element distribution at the interface

The results of area EPMA scanning on the Al and Cu distribution and the BSE image of the interfacial region are shown in Figs. 6(a)-6(c). The result is consistent with the microstructure seen in Fig. 5 and shows that the interface zone is divided into four sub-layers with different thicknesses and morphologies. In addition, at higher magnification (Fig. 6(d)), another sub-layer with 1 μm thickness is found between the $CuAl_2$ layer and the Cu solid, and it is confirmed to be a Cu_9Al_4 phase by EDS analysis.

In order to understand the distribution features of the Cu and Al at the interface of the CCA rod, element content variations of Cu and Al were also detected by EPMA line scanning (Fig. 7). The results indicate that the average Al element content decreases gradually across the interface from the Al side to the Cu side. The variation in the Cu composition follows the opposite trend.

The formation of metallurgical bonds between Al and Cu should include several steps, such as diffusion of Cu into liquid Al, reaction between Al and Cu, partial re-melting of Cu, and then, solidification of Cu. The results indicate that the interdiffusion layer is about 200 μm, suggesting adequate re-melting and infiltration. Meanwhile, the formation of $CuAl_2$ and Cu_4Al_9 indicates sufficient interaction between the Al and Cu. As a result, an excellent metallurgical bond in the bimetal CCA rod is obtained.

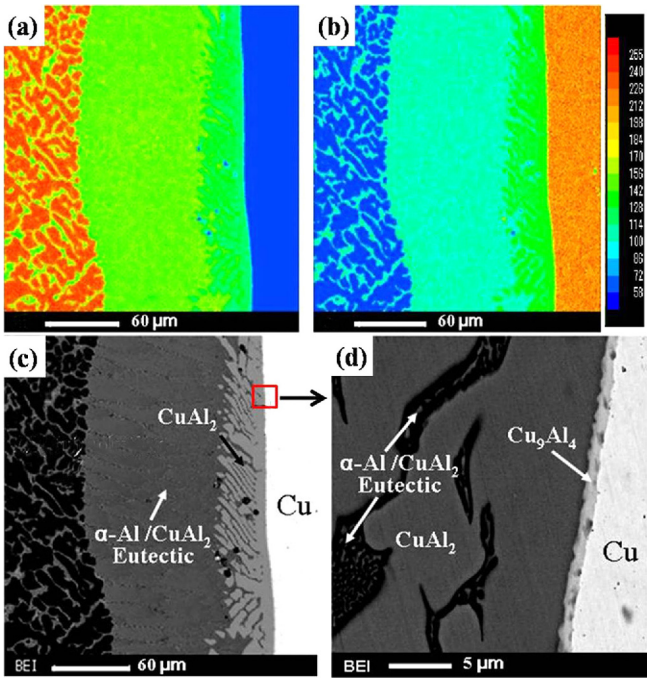

Fig. 6. EPMA analysis at the interface; (a) area scanning of Al and (b) Cu distribution, (c) BSE image, and (d) the magnified region.

3.4. Mechanical properties

Tensile testing is an efficient approach to examine the interface strength. Three samples were selected to evaluate the strength of the interface bonding. A schematic representation of the tensile-shear specimen can be seen in Fig. 8(a). The specimens were cut from the longitude section of the as-cast CCA ingot, and the tensile direction was parallel to the continuous casting direction. The shear strength τ can be calculated by the following equation:

$$\tau = \frac{F}{A} \quad (1)$$

where F is the applied force, and A is the impact area (8×3.5 mm^2 in this study).

Figure 8(b) shows a tensile-shear specimen after testing. It can be seen that the fracture is located in the interface zone. From the microstructure and element distribution analysis above (Figs. 5 and 6), it is seen that a large amount of Al-Cu IMC, including $CuAl_2$ and Cu_4Al_9, is formed at the interface.

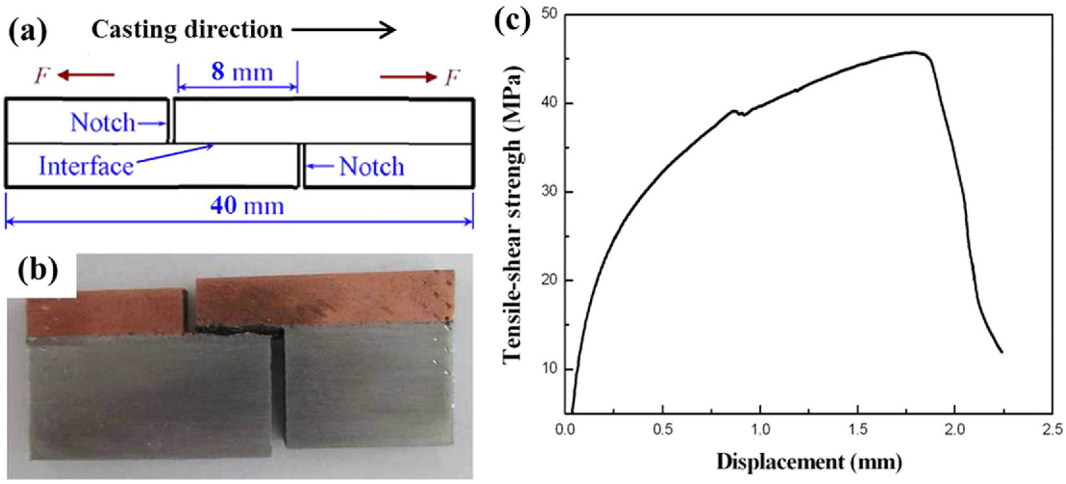

Fig. 8. (a) Schematic illustration of the tensile-shear specimen, (b) the failed tensile-shear sample, and (c) shear strength-displacement curve of the CCA ingot.

The presence of hard IMCs at the interface makes it more brittle in comparison to the plastic Al and Cu sides. In this case, the fracture always occurs in the interface region. It can therefore be considered that the tensile-shear strength of the interface is lower than that of both the Cu and Al sides. However, the results deduced from the shear strength-displacement curve (Fig. 8(c)) suggest that the mean value of the tensile-shear strength is 45 MPa. This is indicative of relatively good bonding strength, which can fulfill the requirements for further extrusion.

4. DISCUSSION

Interdiffusion occurs when liquid Al comes into contact with solid Cu. At the initial stage of this process, IMCs start to form after an incubation period (t_0), which can be expressed by the equation

$$t_0 = k\exp\left[\frac{A+E}{RT}\right] \quad (2)$$

where k is the dissolving constant of the reacting phase, A is the effective activation energy of the reaction, E is the atomic activation energy of the dissolving element, R is the gas constant, and T is the absolute temperature. From Eq. (2), it can be considered that the higher the reaction temperature, the shorter is the incubation period needed to form IMCs at the interface. The growth of an IMC phase is controlled by the diffusion, reaction rate, or both.

The interdiffusion and reaction rate are significantly affected by the contact temperature between the liquid Al and the solid Cu. The higher the contact temperature is, the higher are the diffusion and reaction rates. The optimal contact temperature will ensure appropriate diffusion and reaction rates, as well as moderate re-melting of the Cu layer. Otherwise, casting defects, pores, superfluous re-melting, or even breakage of the Cu layer can be introduced. In other words, control of the re-melting process is the key for successful metallurgical bonding between Al and Cu. As the atoms in the molten Al diffuse into the Cu solid, the composition of Cu changes from pure Cu to Cu-Al alloy in the diffusion region. This causes a significant decrease in the melting point and contributes to the re-melting of the Cu layer.

The heat radiation also facilitates the re-melting of the Cu layer. On the one hand, the reaction between Cu and Al generates heat radiation during the solidification. On the other hand, according to the simulation results, at the initial stage of the solidification process, the direction of heat flow at the interface is from the Cu solid to the Al liquid; this is because the temperature of the Cu solid is higher than that of the Al liquid (Figs. 3 and 4). However, under the strong effect of the cooling water, the actual direction of heat flow within the whole CCA ingot should be from the inside to the outside.

The reaction between Al and Cu will proceed spontaneously as long as the temperature is sufficiently high. According to the binary Al-Cu phase diagram (See ASM Handbook Volume 3: Alloy Phase Diagrams. ASM International Publisher, 1992, P.512), different Al-Cu IMC phases will be formed depending on the concentration of the elements and the cooling rate. For example, when the Cu content ranges between 0 and 5.65%, α-Al (solid solution) forms under the conventional solidification conditions. When the Cu concentration is increased to 53.5%-53.7%, a θ-phase ($CuAl_2$) forms. In the intermediate content region, the eutectic reaction occurs and (α-Al + $CuAl_2$) eutectic precipitates. When the Cu content reaches 79.7%-84%, a γ-phase (Cu_4Al_9) is formed. In this study, the concentration gradient of Al and Cu is caused by the interdiffusion between them; therefore, five layers composed of different phases are observed at the CCA interface, namely, pure Cu, Cu_9Al_4, $CuAl_2$, eutectic (α-Al + $CuAl_2$), and α-Al + eutectic (α-Al + $CuAl_2$).

After the contact of the liquid Al and solid Cu, as the temperature decreases, and solidification starts, first on the Cu side and then on the Al side, due to the strong water cooling effect outside the Cu tube. When the liquid Al comes into contact with the solid Cu, the $CuAl_2$ phase will crystallize immediately at the interface because of the interdiffusion and remelting of Cu and then develop into a layer (block-like shape in Fig. 5(c) arrowed 2) between the Al melt and the Cu solid. The $CuAl_2$ compound is considered the most common IMC in the Al-Cu system, but it is detrimental to the interfacial bonding due to its brittleness. The Cu atoms diffuse continuously from the Cu solid to the Al liquid through the $CuAl_2$ layer. Since there is a small concentration gradient of Cu between the Cu layer and the $CuAl_2$ phase, a 1-μm-thick layer of Cu_4Al_9 is formed at their interface (by the reaction between $CuAl_2$ and Cu). In the meantime, on the Al side, the Cu atoms driven by the effect of the diffusion activation energy can constantly diffuse into the Al melt across the $CuAl_2$ layer. It is found (Fig. 7) that the average Cu content decreases gradually with an increase in the distance from the outer edge, resulting in different reaction products, including a eutectic (α-Al + $CuAl_2$) layer and an α-Al + (α-Al + $CuAl_2$) layer (Figs. 5 and 6). When the casting process reaches the second water cooling stage, the temperature of the CCA rod decreases rapidly, retaining the microstructure, as shown in Fig. 5.

5. CONCLUSION

A high-quality CCA rod with a diameter of 85 mm and a sheath thickness of 16 mm is successfully fabricated by horizontal continuous casting. A good metallurgical bond between the Cu and Al is obtained by this method. The interface between Cu and Al is a multilayered structure with a thickness of 200 μm and consists of Cu_9Al_4, $CuAl_2$, α-Al/$CuAl_2$ eutectic, and α-Al + α-Al/$CuAl_2$ layers. The mean tensile-shear strength of the CCA sample is 45 MPa, which meets the requirements for the next extrusion process.

ACKNOWLEDGEMENT

The authors gratefully acknowledge the support of the National Natural Science Foundation of China (Nos. 51271042 and 51501027), the China Postdoctoral Science Foundation (No.2015M570246), Fundamental Research Funds for the Central Universities of China (DUT15RC(3)065), and the Fundamental Research Funds of Bohai University.

REFERENCES

1. J. K. Kim and T. X. Yu, *J. Mater. Process. Tech.* **63**, 33 (1997).
2. S. Mroz, G. Stradomski, H. Dyja, and A. Galka, *Arch. Civ. Mech. Eng.* **15**, 317 (2015).
3. M. X. Xie, L. J. Zhang, G. F. Zhang, J. X. Zhang, Z. Y. Bi, and P. C. Li, *Mater. Design* **87**, 181 (2015).
4. K. S. Lee, S. Lee, J. S. Lee, Y. B. Kim, G. A. Lee, D. S. Bae, *et al. Met. Mater. Int.* **22**, 849 (2016).
5. M. M. Hoseini-Athar and B. Tolaminejad, *Met. Mater. Int.* **22**, 670 (2016).
6. P. Eslami, A. K. Taheri, and M. Zebardast, *J. Mater. Eng. Perform.* **22**, 3014 (2013).
7. N. Li, S. R. Guo, D. Z. Lu, Z. Q. Hu, and J. L. Wen, *J. Mater. Sci. Technol*. **18**, 187 (2002).
8. E. Takeuchi, M. Zeze, H. Tanaka, H. Harada, and S. Mizoguchi, *Ironmak. Steelmak.* **24**, 257 (1997).
9. K. Y. Rhee, W. Y. Han, H. J. Park, and S. S. Kim, *Mat. Sci. Eng. A* **384**, 70 (2004).
10. L. I. Xiao-Bing, Z. U. Guo-Yin, and P. Wang, *T. Nonferr. Metal. Soc.* **25**, 36 (2015).
11. Y. Fu, J. Jie, L. Wu, J. Park, J. Sun, T. Li, *et al. Mat. Sci. Eng. A* **561**, 239 (2013).
12. H. X. Jiang, H. T. Zhang, K. Qin, and J. Z. Cui, *T. Nonferr. Metal. Soc.* **21**, 1692 (2011).
13. J. C. Benedyk, *Light Met. Age* **64**, 48 (2006).
14. W. Zhang, G. Zou, C. Deng, X. Wei, and X. U. Linkang, *Acta Metall. Sin.* **34**, 609 (1998).
15. N. F. Neumann, U. S. Patent 3421569 (1969).
16. Y. J. Su, X. H. Liu, H. Y. Huang, X. F. Liu, and J. X. Xie, *Metall. Mater. Trans. A* **42**, 4088 (2011).
17. Y. J. Su, X. H. Liu, H. Y. Huang, C. J. Wu, X. F. Liu, and J. X. Xie, *Metall. Mater. Trans. B* **42**, 104 (2011).
18. Z. Yan, X. Li, K. Qi, Z. Cao, X. Zhang, and T. Li, *Mater. Design* **30**, 2072 (2009).
19. N. Liu, J. Jie, Y. Lu, L. Wu, Y. Fu, and T. Li, *J. Mater. Process. Tech.* **214**, 60 (2014).
20. L. Wu, H. Kang, Z. Chen, N. Liu, and T. Wang, *T. Nonferr. Metal. Soc.* **25**, 2675 (2015).